Theoretical Determination of Proton Affinity Differences in Zeolites

G. J. Kramer*,† and R. A. van Santen†,‡

Contribution from the Koninklijke/Shell-Laboratorium, Amsterdam (Shell Research B.V.), P.O. Box 3003, 1003 AA Amsterdam, The Netherlands, and Schuit Institute of Catalysis, Eindhoven University of Technology, P.O. Box 513, 5600 MB Eindhoven, The Netherlands

Received May 21, 1992

Abstract: An important factor in zeolite catalysis is the proton affinity, i.e., the energy required to remove a proton from the zeolite lattice. Differences in proton affinity are expected to influence the catalytic activity of acid sites, making the catalytically active sites inhomogeneous (within one zeolite framework) and dependent on zeolite-framework type. In this study influences of both composition (aluminum content) and structure on proton affinity are examined using both ab initio quantum chemistry and classical force field methods. Changes in the zeolite's aluminum content have a very large influence on the proton affinity of neighboring protons, due to modification of the covalent binding properties of the Si–OH–Al bridge. The structurally induced differences in proton affinity are calculated to be approximately 0.8 eV. These differences in proton abstraction energy can be correlated with structural properties of the all-silica lattice, specifically with the Si–O distances. The zeolites faujasite and ZSM-5 are explicitly discussed.

1. Introduction

Zeolites are widely used as solid acid catalysts in the oil and chemical industries. The acid function is brought about by protons that are attached to the oxygen atoms of the zeolite framework. Catalytic activity is thought to be—at least partially—related to the "intrinsic acid strength" of the protons. At present, a proper definition of "acid strength" for a solid acid is lacking, and its relation to catalytic activity is not well understood. In this paper we will study the intrinsic Brønsted acidity of zeolites and its variation, through the study of proton affinity (the negative of proton binding energy) at different sites within a zeolite lattice. Obviously, equating acidity and proton affinity is a crude approach, since effects like differences in acidic behavior with different conjugate bases are neglected. Nevertheless, gaining insight into the differences in proton binding energy is a vital first step toward a fundamental understanding of zeolite acidity.

Brønsted acidity is influenced by both the chemical composition and by the lattice structure of the zeolite. Chemical influences are manifest in the different acidities of low- and high-aluminum zeolites.[1] It will be shown that the proton is in all cases attached to an oxygen atom bridging an aluminum and a silicon T-atom. The differences are brought about by differences between the aluminum contents of the second coordination sphere of tetrahedral atoms (T-atoms). Structural influences may be inferred from the large variation in catalytic activity that is observed among zeolites that are identical in chemical composition but different in crystal structure. The archetypical examples in this respect are FAU (or faujasite) and ZSM-5 (henceforth MFI), whose catalytic activities may differ by as much as two orders of magnitude in, e.g., hexane cracking.[2]

There exists an extensive body of literature on the subject of the theoretical (viz. quantum chemical) determination of acidity from the proton affinity of small clusters. The T-atoms can be either Si, Al, Ge, Ga, B, or P. Examples of such studies can be found in refs 3–7 and in a review paper by Sauer.[8] One finds that the acidity increases in the order Si–O(H)–B < Si–O(H)–Ga < Ge–O(H)–Al < Al–O(H)–Si, in accordance with experimental evidence. With similar models one can show that two aluminum atoms will avoid neighboring tetrahedra because this is energetically disadvantageous, requiring approximately 1 eV.[9] This accords with the empirical Löwenstein rule, which states that Al-pairing is forbidden.

In this paper we will focus specifically on aluminosilicates by studying—through ab initio quantum chemistry—a total of 12 different aluminosilicate 4-rings, covering all possibilities of aluminum and proton substitution. In this way we can prove the one-to-one coupling between aluminum substituents and protons and rule out the possibility of proton-delocalization, as recently suggested by Derouane et al.[10]

In a preceding paper[11] we presented a force field study that showed that the flexibility of the zeolite framework is quite large and that lattice relaxation upon chemical substitution is important. In particular, zeolitic clusters—the molecular model systems discussed above—are embedded virtually strainlessly. The rationale for this behavior of aluminosilicates lies in the weakness of the Si–O–Si and Al–O–Si angle bending forces. Angles between 130 and 180° are found in natural and synthetic silicas,[12] and it is this flexibility that accounts for both the rich polymorphism and for the ease with which substituents, such as acidic Al–OH groups, can be accommodated in the lattice. In proving the large extent of relaxation within the aluminisilicate lattice, a justification was provided for the use of geometry-optimized (free) clusters, as a reasonable first step toward the modeling of the infinite zeolite lattice.

Although the aluminosilicate lattice is very flexible and relaxation is important, this does not imply that proton affinity is not affected by the crystal environment. The study of the phenomenon of structurally induced differences in proton affinity is more difficult, and less straightforward, than that of chemically induced differences since it requires accurate modeling of the

† Koninklijke/Shell-Laboratorium.
‡ Schuit Institute of Catalysis.

(1) Barthomeuf, D. *Mater. Chem. Phys.* **1987**, *17*, 49–71.
(2) Wielers, A. F. H.; Vaarkamp, M.; Post, M. F. M. *J. Catal.* **1991**, *127*, 51.
(3) Mortier, W. J.; Sauer, J.; Lercher, J. A.; Noller, H. *J. Phys. Chem.* **1984**, *88*, 905.
(4) O'Malley, P. J.; Dwyer, J. *J. Chem. Soc., Chem. Commun.* **1987**, 72.
(5) O'Malley, P. J.; Dwyer, J. *Chem. Phys. Lett.* **1988**, *143*, 97.
(6) Beran, S. *J. Phys. Chem.* **1990**, *94*, 335.
(7) Carson, R.; Cooke, E. M.; Dwyer, J.; Hinchliffe, A.; O'Malley, P. J., preprint.
(8) Sauer, J. *Chem. Rev.* **1989**, *89*, 199.
(9) Hass, E. C.; Mezey, P. G.; Plath, P. J. *Theochem.* **1982**, *87*, 261.
(10) Derouane, E. G.; Fripiat, J. G.; André, J.-M. *Zeolites* **1990**, *10*, 221.
(11) Kramer, G. J.; de Man, A. J. M.; van Santen, R. A. *J. Am. Chem. Soc.* **1991**, *113*, 6435.
(12) Gibbs, G. V. *Am. Mineral.* **1982**, *67*, 421.

0002-7863/93/1515-2887$04.00/0

entire zeolite lattice at a degree of accuracy that is comparable to that of ab initio quantum chemistry.

The same force field parameterization of the acid aluminosilicate lattice as used in ref 11 will be used here to calculate the variation of proton affinity among various crystallographic positions. Zeolites FAU and MFI will be explicitly considered, because of their widely different crystal structures and to facilitate comparison with similar studies that have been published recently by Schröder, Sauer, Leslie, Catlow, and Thomas[13,14] and with earlier work by Dubský et al.[15]

While the gist of most previous work is that chemical compositional influences on acidity dominate over structural influences, we will show that the effects are of similar magnitude. However, due to the fact that protons may occupy any of the four oxygen sites that surround an aluminum substituent, but will occupy only the one that is the lowest in energy, the structural effects on acidity cannot be probed in experiments performed in thermodynamic equilibrium.

The organization of the paper is as follows. In section 2 we explore the chemical influence on proton binding by means of ab initio quantum chemical calculations on geometry-optimized 4-ring clusters. It is found that the proton is invariably bonded to one of the oxygen atoms bridges an aluminum and a silicon atom. Variation of the proton affinity of this bond is induced by changes in the covalent bonding strengths in neighboring atoms. Next (section 3) we study the structural influences on proton binding, by studying zeolites FAU and MFI with force field methods. Special emphasis is given to the reproducibility of results obtained with different force fields. Also, we discuss the origin of the structurally induced variation, which is again the variation in covalent bonding. Finally, we give a brief summary of the results (section 4).

2. Quantum Chemical Calculations: Proton Affinities of Aluminosilicate 4-Rings

In this section we will study the proton affinity differences in zeolites by means of ab initio quantum chemical calculations on small zeolitic clusters. All calculations were performed with the quantum chemistry package GAMESS.[16] As argued before, the flexibility of the zeolite framework ensures that geometry-optimized clusters are appropriate model systems for the study of chemical influences on the proton affinity.

Zeolites (aluminosilicates) form 4-connected networks built from TO_4 (T = Si, Al) tetrahedral units. The chemical composition of $Si_{1-x}Al_xO_2$ 4-connected nets has been found to obey the following (empirical) rules: With formal charges assigned to the atoms, the lattice is either neutral or negatively charged. Charge compensation comes either from mono- or divalent cations such as Na^+ or from protons. Aluminum atoms cannot occupy neighboring tetrahedrons (Löwenstein's rule). Hence the chemical composition of $Si_{1-x}Al_xO_2$ is restricted by

$$0 \le x \le \frac{1}{2} \qquad (1)$$

One of the smallest molecular system that allows for systematic exploration of chemical binding and attachment of protons is the $(TO(OH)_2)_4$ 4-ring depicted in Figure 1. We adopt the following notation to define the rings: $T_1^H T_2 T_3 T_4$ denotes a ring that consists sequentially of T-atoms T_1, T_2, T_3, and T_4; the last is again connected to T_1. The H-superscript indicates the addition

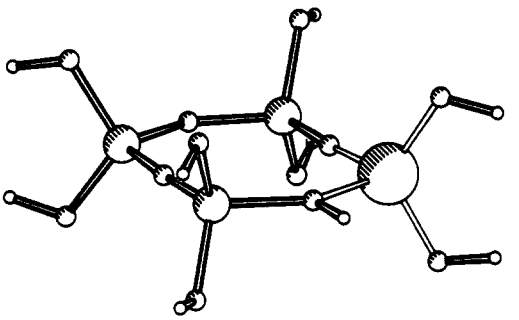

Figure 1. The $[(TO(OH)_2]_4$ 4-rings used in this study. All rings obey at least C_s (mirror) symmetry.

of a proton to the oxygen atom bridging T_1 and T_2. Figure 2 provides a graphical rendering of all 12 4-rings used in this study.

Ab initio quantum chemical calculations on 4-ring clusters were performed at three different levels of sophistication. In all cases the rings are assumed to be flat and to have mirror symmetry in the plane of the ring. These symmetry restrictions ensure rapid convergence of the quantum-chemical geometry-optimization routine to a unique minimum, thereby avoiding problems associated with local minima. A possible disadvantage is that the symmetry-restricted minimum may not be equivalent to the global minimum. However, because of the flexibility of the T–O–T bonds (see, e.g., ref 11), this has only a minor effect on the results. The three different methods of calculation are as follows. Method A: Complete geometry optimization employing a minimal (STO3G) basis set. The core electrons were described by pseudopotentials.[17] During the optimization the terminal OH groups were restricted in such a way that for each T-atom there is a H–O–T–O–H plane. Method B: All-electron split-valence calculations employing a 3-21G basis set. The STO3G-optimized geometry was used, with additional relaxation of the position of the acid proton (both OH distance and H–O–T angle). Method C: Full geometry optimization in the 3-21G basis. The restriction that the H–O–T–O–H group of atoms lie in a plane was lifted. Mirror symmetry in the plane of the 4-ring was retained. The total energies and proton affinities of 4-rings obtained with methods A, B, and C are tabulated in Table I.

Table I shows that the proton affinities of the various 4-rings span a considerable energy range. Also, the absolute proton affinity (PA) values appear to depend on the method chosen. As the chief interest is in trends in the proton affinity, we may focus on PA differences rather than on absolute values. The trends in PA are predicted identically for all methods, in which the correlation coefficient exceeds 0.98. This indicates that the "chemistry is right", even when using the STO3G basis set. The 3-21G results compare satisfactorily with previous ab initio work.[8]

To study chemical influences on PA, it is useful to present the data of Table I in a different way, by ordering the PA values according to the type of oxygen that is (de)protonated and according to the charge of the protonated cluster. Table II displays the proton affinities as a function of the protonated bond and the charge of the protonated cluster. A further refinement is made by an additional ordering with respect to the chemical nature of the 4-ring, i.e., low- or high-aluminum. As shown by the middle column of this table, the proton affinity is strongly modified by the chemical nature of the T-atoms that coordinate the protonated oxygen atom.

The proton affinity is highest for the Al–O–Si bridge: over 2 eV higher than that of the Si–O–Si bond, so the proton is necessarily localized on the Al–O–Si bond. This observation is of prime importance since it implies that acidity differences as observed between different zeolites are due to differences between

(13) Schröder, K.-P.; Sauer, J.; Leslie, M.; Catlow, R. C. A.; Thomas, J. M. *Chem. Phys. Lett.* **1992**, *188*, 320.
(14) Schröder, K.-P.; Sauer, J.; Leslie, M.; Catlow, R. C. A. *Zeolites* **1992**, *12*, 20.
(15) Dubský, J.; Beran, S.; Bosáček, V. *J. Mol. Catal.* **1979**, *6*, 321.
(16) Dupuis, M.; Sprangler, D.; Wendolowski, D. *NRCC Software Catalog*; 1980; Vol. 1, Program No. QG01, GAMESS. Guest, M. F.; Kendrick, J. *GAMESS User Manual, An Introductory Guide*; 1986; CCP/86/1, Daresbury Laboratory.
(17) Barthelat, J. C.; Durand, P. H.; Serafina, A. *Mol. Phys.* **1977**, *33*, 159.

Low-aluminum zeolitic clusters

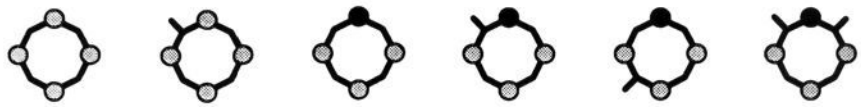

1: SiSiSiSi 2: $Si^{H}SiSiSi$ 3: AlSiSiSi 4: $Al^{H}SiSiSi$ 5: $AlSi^{H}SiSi$ 6: $Al^{H}SiSiSi^{H}$

High-aluminum zeolitic clusters

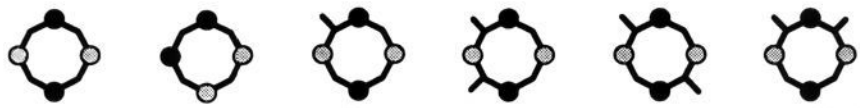

7: AlSiAlSi 8: AlAlSiSi 9: $Al^{H}SiAlSi$ 10: $Al^{H}Si^{H}AlSi$ 11: $Al^{H}SiAl^{H}Si$ 12: $AlSi^{H}Al^{H}Si$

Figure 2. Enumeration of all 12 4-rings studied in this paper. The solid circles indicate $T(OH)_2$ groups; protons are indicated by sticks protruding from the oxygen atoms that are part of the ring.

Table I. Total Energies (in Atomic Units) and Proton Affinities (in eV) of 4-Ring Clusters[a]

		A: STO3G (optimized geometry)		B: 3-21G (STO3G geometry)		C: 3-21G (optimized geometry)	
	ring	*E* (au)	PA (eV)	*E* (au)	PA (eV)	*E* (au)	PA (eV)
1	SiSiSiSi	−203.318 558		−2048.522 833			
2	$Si^{H}SiSiSi$	−203.779 993	12.56	−2048.839 850	8.63		
3	AlSiSiSi	−201.331 399		−2001.777 284		−2001.850 643	
4	$Al^{H}SiSiSi$	−202.002 739	18.27	−2002.279 709	13.67	−2002.374 317	14.25
5	$AlSi^{H}SiSi$	−201.925 292	16.16	−2002.208 117	11.72	−2002.309 532	12.49
6	$Al^{H}SiSiSi^{H}$					−2002.749 718	10.22*
7	AlSiAlSi	−199.216 525		−1954.926 577		−1954.988 098	
8	AlAlSiSi	−199.161 940		−1954.885 995			
9	$Al^{H}SiAlSi$	−200.024 318	21.98	−1955.542 784	16.77	−1955.626 118	17.36
10	$Al^{H}Si^{H}AlSi$	−200.633 693	16.58*	−1955.994 844	12.29*	(−1956.120 927	13.46*)
11	$Al^{H}SiAl^{H}Si$	−200.726 481	19.10*	−1956.067 643	14.27*	−1956.163 893	14.63*
12	$AlSi^{H}Al^{H}Si$	−200.683 936	17.94*	−1956.024 463	13.11*	−1956.125 167	13.58*

[a] Complete geometry optimizations were performed at the STO-3G level; the 3-21G results refer to the STO3G-optimized geometry with an additional optimization of the proton position. Results marked by an asterisk refer to the abstraction of one proton only; the result in parentheses is influenced by a different configuration of the terminal hydrogen atoms; the results in italics refer to a configuration that violates Löwenstein's rule.

Table II. Proton Affinities (eV) of 4-Rings Obtained with Method B, Grouped According to Oxygen Type and Cluster Charge[a]

protonated bond		charge of protonated cluster		
		−1	0	1
Al–O–Si	HAZ	17.36	14.63	
	LAZ		14.25	10.22
Si–O–Si	LAZ		12.49	

[a] HAZ is high-aluminum zeolite; LAZ is low-aluminum zeolite.

the acidic properties of the Al–OH–Si unit. Differences that may be—as said—either chemical or structural.

A further restriction is imposed by what seems to be a requirement of "local charge compensation", by which we mean that the formal charge excess of each aluminum substituent in a zeolite has to be compensated locally by a proton through its attachment to a neighboring oxygen atom. This requirement can be inferred from the comparison of the energies in Table I of two ring-4 species ($Al^{H}SiSiSi$) with rings 3 and 6 (AlSiSiSi and $Al^{H}SiSiSi^{H}$). This disproportionation of aluminum and charge balancing protons requires approximately 4 eV. In an actual zeolite, this effect may be screened by the polarizable lattice, but a considerable energy penalty is expected to remain. A similar effect is seen for the various arrangements of two protons in a high-aluminum ring (configurations 10, 11, and 12). Here, the configuration that has the protons farthest apart (number 11) is favored by more than 1 eV (methods B and C) over other configurations that have two protons next to one T-atom (numbers 10 and 12).

Apart from this dependence on the chemical composition of the first shell of T-atoms, we may examine the PA differences between low- and high-aluminum zeolites in the same fashion, by substituting Al–OH–Si for Si–O–Si (changing configuration 4 into 11). The increase in PA is 0.4–0.6 eV (methods C and B, respectively), whence it is concluded that the intrinsic acidity decreases with increasing aluminum concentration, in accordance with experiment.[1]

Extrapolating these results to extended systems (zeolites), it seems likely that chemically induced differences may be even larger for extended systems than for these clusters, since, in the study of 4-rings, only two out of a possible total of six T-atom neighbors are substituted. A first estimate would be that chemical differences, such as those between, e.g., low-aluminum zeolites and high-aluminum zeolites, lead to proton affinities that may differ by as much as 1 eV.

Although the notation "acid proton" would suggest a considerable ionicity of the bond, the acidic OH chemical bond is actually quite covalent, as is evident from a number of theoretical observations in a paper by one of us:[18] firstly, the Mulliken charge on the "acid proton" is typically 0.20 at the STO3G level, as compared to 0.13 for the hydrogen atoms of the terminal OH groups. It was also found that addition of a proton to a negatively charged zeolite cluster causes markedly different distortions of this cluster as compared to the addition of a Na^+ ion. Specifically, the sodium ion occupies a symmetrical position close to the (negatively charged) AlO_4 tetrahedron, whereas the proton forms a bond with one of the oxygen atoms, thereby breaking the symmetry. In ref 18 it was shown that the changes in the TO bond lengths upon protonation can be explained by the principle of bond order conservation, which again calls on the covalent nature of the OH bond. In this work, additional evidence for the covalent character of the acidic OH bond is provided by the fact

(18) van Santen, R. A.; van Beest, B. W. H.; de Man, A. J. M. In *Guidelines for Mastering the Properties of Molecular Sieves*; Barthomeuf, D., Ed.; Plenum: New York, 1990; p 201.

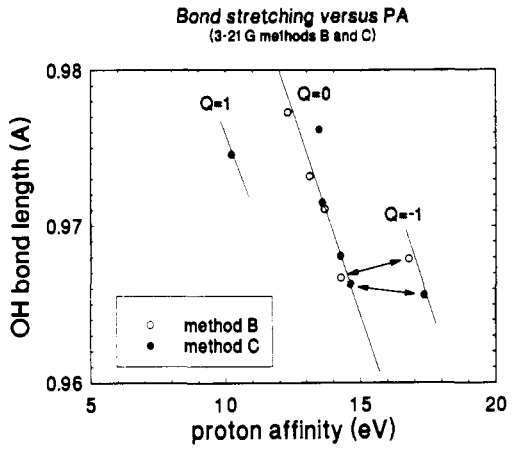

Figure 3. The OH bond length versus the proton affinity for protons attached to Al–O–Si oxygen atoms. The arrows connect configurations 11 ($Q = 0$) and 9 ($Q = -1$), which are both high-aluminum models. As a consequence of the covalent character of the OH chemical bond, its length is not affected by the cluster charge.

that the OH bond length decreases as the bond strength (as measured by PA) increases. Figure 3 shows the dependence of the OH bond length on PA for all Al–OH–Si bonds, for which one observes a linear relationship. Also, comparing the OH bond lengths of high-aluminum clusters with one or two protons (configurations 9 and 11), one observes that the bond length does not vary upon a change in the charge of the cluster as one would expect for an ionic bond.

In summary, we have found that acid protons form the strongest bond with oxygen atoms that form a bridge between Al and Si T-atoms. Proton binding to an oxygen atom with other T-atom neighbors in weaker by more than 2 eV. Hence, protons are invariably localized on Al–O–Si units. The acidity of this unit is influenced by chemical composition of the second sphere of T-atoms, making low-aluminum zeolites more acidic than high-aluminum zeolites. Such modification of the proton affinity of the Si–O–Al bond is a covalent process, which is rationalized on the basis of the bond order conservation principle.

3. Molecular Mechanics Calculations: Proton Affinity Differences in Zeolites FAU and MFI

In this section we will present and discuss results of a force field study of periodic zeolites. The force field that describes the interatomic interactions is written as a sum of classical potential energy functions, dependent on interatomic distances and angles. Its parametrization has been described previously[19,20,11] and is optimized to fit both the potential energy surfaces of small aluminosilicate clusters, as calculated by ab initio quantum chemistry, and the (experimentally determined) structural and elastic properties of quartz. The energy minimization scheme has been described in the literature.[21]

To simplify matters, we have decided to describe the acid OH group as an effective atom, denoted by O_H. The potential energy functions (ϕ) that define the force field are the sum of the long-range Coulomb interactions and short-range interaction described by a Buckingham potential

$$\phi_{ij}(r_{ij}) = \frac{q_i q_j}{r_{ij}} + A_{ij}\exp(-b_{ij}r_{ij}) - \frac{c_{ij}}{r_{ij}^6} \qquad (2)$$

where i,j run over all atoms, q_i denotes effective charge, and A_{ij}, b_{ij}, and c_{ij} are short-range parameters that depend on the atom types of atoms i and j. Additionally, a three-body term has been introduced to describe the Al–O_H–Si bond bending

$$\phi_{ijl}(\theta_{ijl}) = \frac{1}{2}k_{ijl}(\theta_{ijl} - \theta_0)^2 \qquad (3)$$

with k_{ijl} and θ_{ijl} as parameters.

Beside parametrizations of the protonated zeolite, we have made additional parametrizations for the bare aluminosilicate lattice, where it is assumed that the compensating charge of the silicon–aluminum substitution is spread out evenly over all remaining silicon atoms. All force field parameters used in this study are given in Table III. They are the same as in ref 11 with the addition of two sets that have been derived to allow for the modeling of the bare ($AlSi_{95}O_{192}$) MFI unit cell.

Even though protons are not treated as separate entities in the calculations, this approach still allows for the determination of PA *differences* by comparing the energy of replacement of O by O_H at different sites. In the following we will consider periodic systems with one acid AlO_H group per unit cell.

The results were obtained using four different force field descriptions of the aluminosilicate lattice. These variations will be used to rule out systematic errors in the final results. Two different choices are made for the charge *difference* between Al and Si (and hence between O and O_H), namely 1 and 0.5 times the electron charge. This variation allows us to probe the sensitivity of results for changes in the "ionicity" of the force field, which is, as argued in earlier papers,[20,22] not uniquely defined.

A second test for the stability of results is obtained by so-called truncation of the short-range part of both of the above force

Table III. Force Field Parameters Employed in This Study[a]

species α_i–α_j	short-range parameters $A_{\alpha_i\alpha_j}$ (eV)	$b_{\alpha_i\alpha_j}$ (Å^{-1})	$C_{\alpha_i\alpha_j}$ (eV Å^6)	q_α
O–O	1388.773 0	2.760 00	175.000 0	$q_O = -1.20$
O–O_H	9747.010 5	3.879 92	175.000 0[b]	$q_{O_H} = -0.20$
O_H–O_H			175.000 0	
Si–O	18003.757 2	4.873 18	133.538 1	$q_{Si} = 2.40$
Si–O_H	26949.728 5	5.038 88	176.694 1	
Al–O	15430.443 4	4.815 06	130.851 6	$q_{Al} = 1.40$
Al–O_H	9419.858 5	4.510 28	102.858 9	
Si–O_H–Al	$k = 0.5334$ eV·rad^{-2}, $\theta_0 = 88.62°$			
O–O	1388.773 0	2.760 00	175.000 0	$q_O = -1.20$
Si–O	17679.585 6	4.868 48	131.188 9	$q_{Si} = 2.42$
Al–O	14630.331 7	4.802 87	124.281 8	$q_{Al} = 1.46$
O–O	1388.773 0	2.760 00	175.000 0	$q_O = -1.20$
Si–O	17841.806 3	4.870 83	132.364 6	$q_{Si} = 2.41$
Al–O	14764.317 7	4.804 99	125.384 3	$q_{Al} = 1.45$
O–O	1388.773 0	2.760 00	175.000 0	$q_O = -1.20$
O–O_H	37139.895 0	4.655 93	175.000 0[b]	$q_{O_H} = -0.70$
O_H–O_H			175.000 0	
Si–O	18003.757 2	4.873 18	133.538 1	$q_{Si} = 2.40$
Si–O_H	14031.838 8	4.790 33	101.058 3	
Al–O	8566.543 4	4.662 22	73.091 3	$q_{Al} = 1.90$
Al–O_H	3237.507 9	4.053 60	32.285 6	
Si–O_H–Al	$k = 0.7099$ eV·rad^{-2}, $\theta_0 = 88.42°$			
O–O	1388.773 0	2.760 00	175.000 0	$q_O = -1.20$
Si–O	17841.755 1	4.870 84	132.364 7	$q_{Si} = 2.41$
Al–O	8149.848 5	4.647 34	69.441 1	$q_{Al} = 1.93$
O–O	1388.773 0	2.760 00	175.000 0	$q_O = -1.20$
Si–O	17922.828 5	4.872 01	132.951 6	$q_{Si} = 2.405$
Al–O	8219.215 8	4.649 89	70.050 5	$q_{Al} = 1.925$

[a] The terms between blank lines are internally consistent sets. The first and fourth are used for modeling of protonated zeolites, with $\delta Q = 1$ and 0.5, respectively; the others are used for the study of aluminum substitution energies with Si:Al ratios of 47 (FAU) and 95 (MFI). It is assumed that the compensating charge is homogeneously redistributed over all silicon atoms. Here again, we have $\delta Q \approx 1$ and 0.5. [b] Fixed during optimization.

(19) van Beest, B. W. H.; Kramer, G. J.; van Santen, R. A. *Phys. Rev. Lett.* **1990**, *64*, 1955.
(20) Kramer, G. J.; Farragher, N. P.; van Beest, B. W. H.; van Santen, R. A. *Phys. Rev.* **1991**, *B43*, 5068.
(21) Catlow, C. R. A.; Mackrodt, W. C. In *Computer Simulation of Solids*, *Lecture Notes in Physics* 66; Catlow, C. R. A., Mackrodt, W. C., Eds.; Springer: Berlin, 1982.
(22) Kramer, G. J.; van Santen, R. A.; van Beest, B. W. H. *Nature* **1991**, *351*, 636–638.

Table IV. Force Field Results on the O_H Substitution Energy in FAU[a]

	force field (δQ = 1)					
	relaxed structure				SiO_2 structure truncated	
O_H site	full range		truncated			
O_1	−2737.3914	0.35	−2737.2426	0.13	−2734.1208	0.04
O_2	−2737.0744	0.67	−2736.8951	0.47	−2733.7115	0.36
O_3	−2737.7415	0	−2737.3684	0	−2734.0746	0
O_4	−2736.9733	0.87	−2736.7716	0.60	−2733.6932	0.38

	force field (δQ = 0.5)			
	full range		truncated	
O_H site				
O_1	−2745.5870	0.52	−2745.9527	0.44
O_2	−2745.2037	0.91	−2745.5649	0.82
O_3	−2746.1145	0	−2746.3898	0
O_4	−2745.0117	1.10	−2745.2805	1.11

[a] Both absolute and relative values are given in eV. Results are presented for formal and half formal charge *differences* (see Table III), and for full-range O_H potentials and truncated ones, the meaning of which is discussed in the text.

Table V. Comparison of Our (Averaged) Results with Those by Schröder et al.[13] and Dubský et al.[15] [a]

		theoretical energy predictions			
		relaxed structure		fixed structure	
O_H site	expt (fractional occupancy)	this work (ff, av)	Schröder (ff)	this work (ff)	Dubský (CNDO/2)
O_1	0.23 ± 0.06	0.36	0.05	0.05	0.07
O_2	0	0.74	0.21	0.36	0.40
O_3	0.34 ± 0.08	0	0	0	0
O_4	0	0.92	0.25	0.38	0.60

[a] The neutron diffraction data on proton distribution by Jirák and co-workers[24] are also given.

fields. By truncation we mean the limiting of the range of the short-range force field description of O_H and Al substituents to interactions with neighboring Si and O atoms to 3.5 Å. Beyond this range we replace the short-range interaction of O_H by that of a regular O atom and that of Al by Si. Truncation thus implies that beyond nearest neighbor distances the AlO_H substituent is indistinguishable from an SiO pair, except for its charge. In doing so, we can probe the sensitivity of our results with respect to changes in the medium range (3.5–10 Å) description of the force field. Over this range of distances, interactions are least well defined as a consequence of the force field derivation procedure which is based on calculations on small (dimer) clusters. In Appendix I we give a detailed account of the effect of truncation.

In this section we will often speak about relative proton energies; the energy of an O_H substitution is proportional to the negative of the proton affinity of that site and is calculated as: $E(\text{proton}) = E(AlO_H) - E(Al)$.

3.1. Proton Affinity Differences in Faujasite. Faujasite is a zeolite with a very large, highly symmetric, cubic unit cell comprising 192 T-atoms. There is only one unique T-atom surrounded by four different oxygen atom types (see Figure 4). In our calculations we used a smaller, noncubic representation of the unit cell with 48 T-atoms, $a = b = c \approx 17.5$ Å and $\alpha = \beta = \gamma = 60°$. Calculations thus refer to an Si:Al ratio of 47.

Tables IV and V provide a compilation of AlO_H substitution energies obtained in this study. In Table V a comparison is made with results which Schröder et al.[13] obtained by means of lattice minimization of the FAU lattice using an empirical force field parametrization. Also, we quote results by Dubský et al.[15] as obtained from CNDO/2 calculations on clusters with an "experimental" geometry. As the latter results are obtained for "strained" clusters, i.e., clusters that have the geometry of the all-silica lattice, we have included for comparison a set of force field results on the unrelaxed AlO_H substitution energy in FAU, using the force field-optimized geometry of the all-silica form.

Within all sets of calculations, O_3 is predicted to be the energetically favored site. One observes that the ordering of sites according to energy (3, 1, 2, 4) is the same for all approaches. Also, these theoretical results accord with the outcome of neutron diffraction experiments by Olson[23] and Jirák et al.,[24] who find proton occupancies for sites 3 and 1, but not for sites 2 and 4. [A more recent study by Jobic et al.[25] also showed protons at the O_2 site. This is likely due to the presence of sodium ions in the double 6-ring in their faujasite samples; the studies by Olson and Jirák were performed on completely protonated faujasite.]

Within all data sets, a clear correlation between proton energies and the nearest neighbor TO_H distances was found (Table VI): the longer the TO_H distances, the better the proton is accommodated, i.e., the lower the proton energy. The constant of proportionality is approximately 10 ± 5 eV/Å, which seems reasonable in its implication that compression of a TO_H bond by 0.1 Å results in 1 eV difference in proton binding energy. Below (in section 3.3) we will discuss this correlation further and analyze its origin.

While the ordering of energies is identical for all approaches, there are considerable variations in the absolute magnitude of the differences. These are listed in Table VII as the root mean square (RMS) width of the energy distribution, defined as

$$W_{RMS} = 2\langle (E - \langle E \rangle)^2 \rangle^{1/2} \quad (4)$$

By studying these changes in association with the variation of the force field, we see that the PA differences are not induced by electrostatic interaction. The width of the distribution increases slightly as the charge difference of the substituents is increased, indicating that the differences do not arise as a consequence of electrostatic interactions. The truncation of the force field, which probes the effect of varying descriptions at intermediate ranges, leads to a small, but systematic, decrease in the predicted energy differences. Both observations lead us to conclude that the variations of the proton energy as a function of crystallographic site are real, and can be correlated with experimental data.

3.2. Proton Affinity Differences in MFI. MFI is a zeolite that is crystallographically very different from FAU.[26] It has medium size (10-ring) pores and no cavities, and the framework is built almost entirely from 5-rings rather than from 4- and 6-rings as in FAU. Additionally, MFI is, in a crystallographic sense, a much more complex zeolite than FAU. It has 12 topologically different T-sites and 26 different O-sites. Of these 26 different oxygen atoms, 22 atoms bridge crystallographically different T-atoms; 4 atoms (oxygen sites 23–26) bridge T-atoms that are symmetry-related. This yields a total of 48 different possibilities for Al–O_H substitution. Although a recent structure refinement[27] indicated that the low-temperature structure is actually monoclinic, we will use the high-temperature ($T > 340$ K) monoclinic structure as a starting point, firstly to reduce the number of possible configurations, and secondly because this is the structure that is of prime interest for catalysis.

As proton affinity is the energy required for the removal of a proton, it is the energy difference between the protonated and the unprotonated zeolite. Hence, while proton affinity differences of oxygen atoms near the same aluminum substituent can be read immediately from the AlO_H energies—as done for faujasite—the proton affinity differences between oxygen atoms near different crystallographic T-sites are influenced by the differences in

(23) Olson, D. H.; Dempsey, E. *J. Catal.* **1969**, *13*, 221.
(24) Jirák, Z.; Vratislav, V.; Bosáček, V. *Phys. Chem. Solids* **1980**, *41*, 1089.
(25) Czjzek, M.; Jobic, H.; Fitch, A. N.; Vogt, T. *J. Phys. Chem.* **1992**, *96*, 1535.
(26) Olson, D. H.; Kokotailo, G. T.; Lawton, S. L.; Meier, W. M. J. *J. Phys. Chem.* **1981**, *85*, 2238.
(27) van Koningsveld, H.; Jansen, J. C.; van Bekkum, H. *Zeolites* **1990**, *10*, 235.

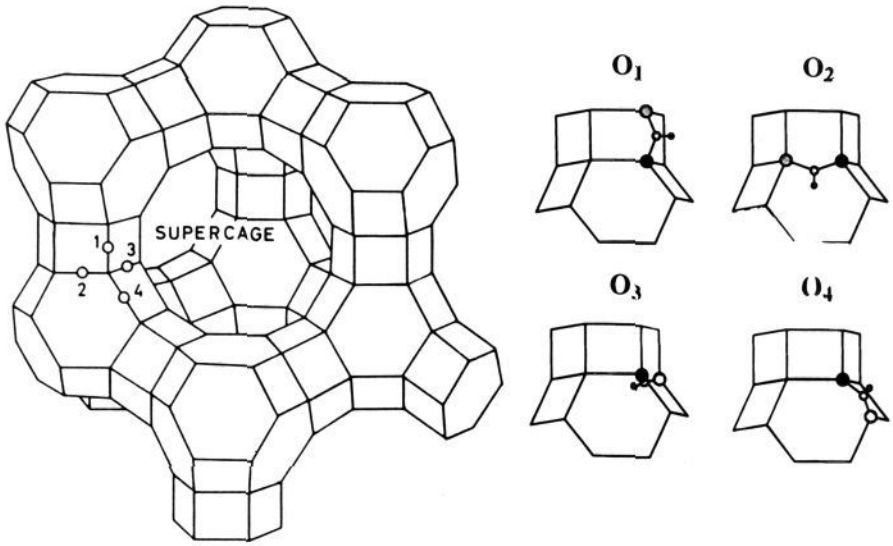

Figure 4. Crystal structure of zeolite FAU, showing the four different oxygen atoms. The small pictures show the positions of the protons attached to each of the oxygen sites around the Al substituent (●), constructed by assuming the proton to be in the Al–O_H–Si plane (after ref 13).

Table VI. Correlation Coefficients r^2 between Energies and Distances Computed or Used in Different Methods[a]

			energies				Σ distances			
			relaxed		fixed		relaxed		fixed	
			this work	Schröder	this work	Dubský	this work	Schröder	this work	Dubský
E	r	ff	1	1.00	0.97	0.98	0.93			
		S	1.00	1	0.99	0.97		0.78		
	f	ff	0.97	0.99	1	0.94			0.98	
		D	0.98	0.97	0.94	1				0.98
Σ	r	ff	0.93				1	0.91	0.79	0.94
		S		0.78			0.91	1	0.64	0.76
	f	ff			0.98		0.79	0.64	1	0.94
		D				0.98	0.94	0.76	0.94	1

[a] The results marked Schröder and Dubský are from refs 13 and 15, respectively.

Table VII. Root Mean Square Width of the Proton Energy Distribution (in eV) in Faujasite and ZSM-5, as a Function of the Force Field

	$\delta Q = 1.0$		$\delta Q = 0.5$	
zeolite	full range	truncated	full range	truncated
FAU	0.76	0.56	0.97	0.96
ZSM-5	0.45	0.24	0.88	0.51

aluminum substitution energy. These are calculated from the energies of bare aluminosilicate lattices, by distributing the compensating charge of the aluminum substitution over all remaining silicon atoms. In this way one can probe the site dependence of the aluminum substitution energy, without being hampered by interference of specific cation locations.

Calculations were performed on a periodic MFI lattice with one aluminum atom per unit cell (Si:Al = 95). The excess charge introduced by the replacement of a silicon atom (q = 2.40) by an aluminum atom (q = 1.45 or 1.925) is spread out over the lattice by a slight increase in the silicon charge (q = 2.41 or 2.405). With these force fields (tabulated in Table III) unrestricted lattice-energy minimizations were performed. Results of total energy calculations are tabulated in Tables VIII and IX. Figure 5 shows the relative substitution energies of aluminum at the 12 different T-sites of ZSM-5. The differences are up to 0.4 eV, and scale with the charge difference between silicon and aluminum. Also, the energy differences between the T-sites correlate well with the value of the local Madelung potential. Both observations indicate that the aluminum substitution energy is dominated by long-range electrostatic effects. This might also explain the discrepancy between our results and those of Fripiat et al., who calculated the substitution energy on the basis of

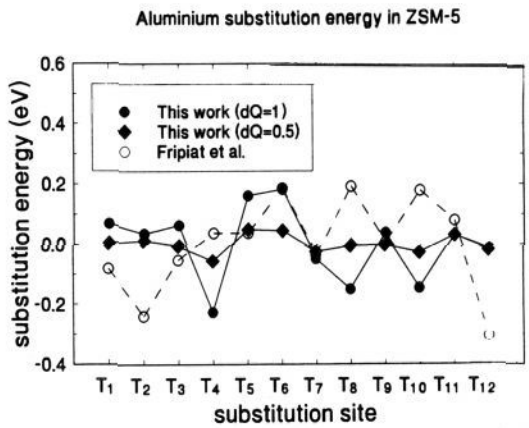

Figure 5. Relative aluminum substitution energies at the 12 different T-sites of orthorhombic MFI for two different force fields, having 0.48 and 0.96 e charge differences between the aluminum and silicon atoms. Results obtained previously by Fripiat et al.[28] are also shown. The discrepancy is discussed in the text.

quantum chemical calculations of small clusters of "experimental" geometry.[28] In such an approach one neglects both lattice relaxation and electrostatic effects.

For all 48 possible AlO_H configurations lattice energy minimizations have been performed using the same sets of force fields as before. It appeared to be necessary to fix the unit cell vectors, since otherwise the unit cell changed in different and unpredictable ways, thereby prohibiting a good comparison of substitution

(28) Fripiat, J. G.; Berger-André, F.; André, J.-M.; Derouane, E. G. *Zeolites* **1983**, *3*, 306.

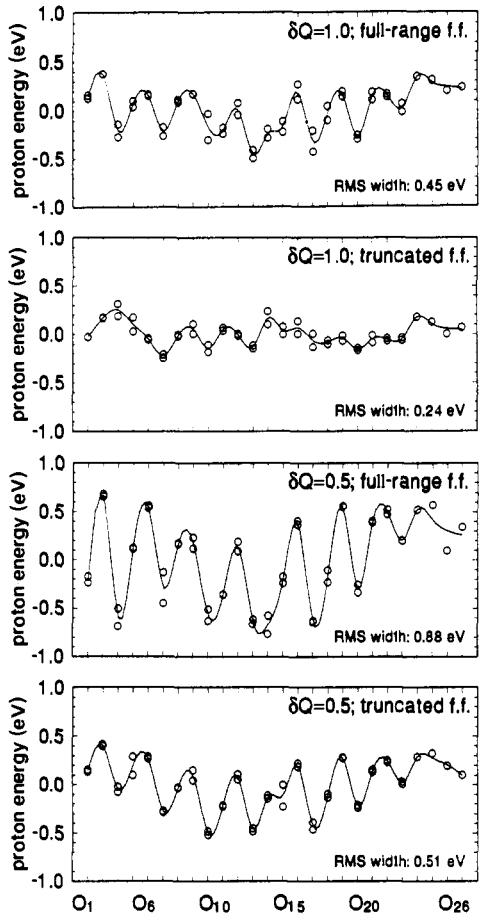

Figure 6. Relative proton energies in MFI, as a function of the protonated oxygen site, for four different force fields. Sites 1–22 have two crystallographically different T-atom neighbors. These two realizations yield slightly different energies. The solid curve is a guide to the eye.

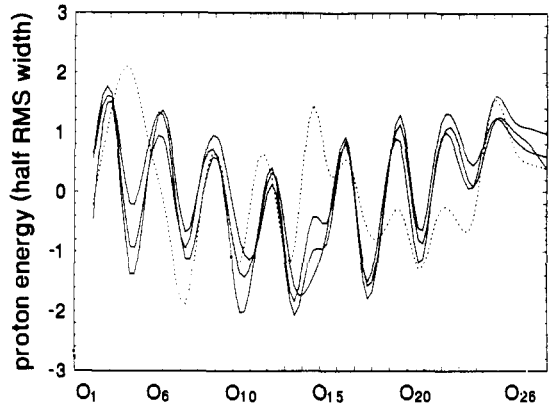

Figure 7. The site dependence of proton energy (scaled to the width of the distribution) for all four force fields. Note the close correspondence between the solid curves (corresponding to the force field: δQ = 1, full-range; δQ = 0.5, full range, and δQ = 0.5, truncated). The δQ = 1, truncated force fields, indicated by the broken curve, deviates, possibly due to numerical inaccuracy.

energies. Results are tabulated in Tables VIII and IX; the RMS values of the proton energy distribution are given in Table VII.

Figure 6 shows a graphical representation of the proton energies as a function of the oxygen site. As most oxygen sites (1–22) bridge different T-atoms, there are two proton energies, corresponding to substitution of aluminum at either of these T-sites. Note that the proton energy is hardly influenced by which of the two T-sites is substituted. As these two realizations differ in the direction of the AlO_H dipolar moment within the lattice, the absence of influence on the proton energy corroborates the

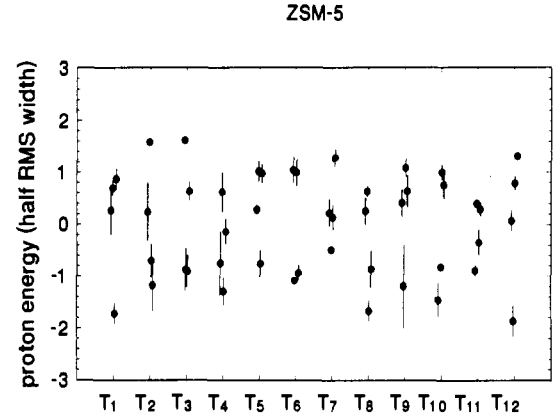

Figure 8. Averaged and scaled proton energies, plotted versus the aluminum-substituted T-site position.

hypothesis that proton energy differences are not determined by electrostatic interactions. The dependence of the width of the distribution (Table VII) on the "ionicity" of the force field shows the same trend as for faujasite; the effect of truncation is also similar, although more pronounced.

It appeared that the predictions made with the different force fields correlate quite well with each other. Figure 7 shows the O-site dependence of the proton energy for all force fields, scaled to the RMS width of the distribution. Three out of four data sets overlap completely in this picture; only the results of the δQ = 1.0 truncated force field shows a discrepancy. This may be attributed to the small absolute value of the width of the energy distribution, which enhances the effect of random fluctuations due to computational inaccuracy.

In most of the following we will use averaged data for the proton energies in MFI. Proton energy data obtained with the three well-correlated force fields have been scaled to their respective RMS width and subsequently averaged. Apart from the average, we also indicate the statistical error, as estimated from the spread between the three data sets. Figure 8 shows these results, plotted versus the T-site which is aluminum-substituted.

A study of proton energies in MFI, similar to ours, has been performed by Schröder et al.,[14] who used the same approach as in their study of faujasite, which we referred to earlier. While their results for FAU yielded the same preferential positions as our calculations, the results for MFI differ markedly from ours. They report explicitly the location of the nine most favored AlO_H substitutions. Comparison with our results shows that the results are essentially uncorrelated. Apart from the fact that the two results have been obtained with entirely different force fields, the discrepancy may be attributed to several facts. Firstly, Schröder et al. use the low-temperature, monoclinic structure as a starting point, whereas we have used the high-temperature, orthorhombic structure. [As the monoclinic–orthorhombic transition temperature is 340 K, the orthorhombic structure will be of most relevance to catalytic properties.] Secondly, they calculate the energy of an impurity in an infinite lattice, which is only locally distorted, whereas we calculate the properties of a periodic system with one substitution per unit cell. Finally, the width of the distribution of Schröder et al. is quite small (RMS width of 0.15–0.25 eV), which may cause random numerical errors to influence the results, as in our case for the δQ = 1, truncated force field.

In conclusion, the reliable prediction of proton energies proved a more difficult task for MFI than for FAU. The spectrum of differences in PA is in all cases similar to that observed in faujasite. The relative insensitivity of results to force field variation suggests that the assignment of high or low PA to specific oxygen sites is possible with the present set of force fields.

3.3. Relation between Proton Energy and Structure. In the previous two sections attention was focused on the reliability of

Table VIII. Force Field Results on the Al and Al-O_H Substitution Energy in MFI[a]

substitution site		force field (dQ = 1)					
		full range			truncated		
Al	O_H	E(Al)	E(Al-O_H)	-PA	E(Al)	E(Al-O_H)	-PA
1	1	-5554.18	-5532.46	0.13	-5554.21	-5532.32	-0.03
	15		-5532.48	0.11		-5532.29	0.00
	16		-5533.02	-0.43		-5532.43	-0.13
	21		-5532.46	0.14		-5532.36	-0.07
2	1	-5554.21	-5532.46	0.16	-5554.24	-5532.35	-0.02
	2		-5532.25	0.38		-5532.15	0.17
	6		-5532.79	-0.17		-5532.54	-0.21
	13		-5532.91	-0.28		-5532.22	0.10
3	2	-5554.20	-5532.24	0.37	-5554.23	-5532.15	0.17
	3		-5532.88	-0.27		-5532.13	0.19
	19		-5532.91	-0.30		-5532.48	-0.17
	20		-5532.50	0.11		-5532.40	-0.09
4	3	-5554.45	-5533.00	-0.14	-5554.49	-5532.25	0.32
	4		-5532.76	0.10		-5532.40	0.17
	16		-5533.07	-0.21		-5532.57	0.01
	17		-5532.82	0.04		-5532.64	-0.06
5	4	-5554.08	-5532.45	0.04	-5554.11	-5532.16	0.03
	5		-5532.32	0.17		-5532.23	-0.04
	14		-5532.71	-0.22		-5532.19	-0.00
	21		-5532.32	0.17		-5532.23	-0.04
6	5	-5554.08	-5532.33	0.16	-5554.11	-5532.25	-0.05
	6		-5532.75	-0.26		-5532.44	-0.25
	18		-5532.35	0.15		-5532.26	-0.07
	19		-5532.75	-0.26		-5532.34	-0.14
7	7	-5554.30	-5532.62	0.09	-5554.33	-5532.41	-0.00
	17		-5532.81	-0.10		-5532.51	-0.10
	22		-5532.73	-0.02		-5532.47	-0.06
	23		-5532.37	0.34		-5532.23	0.18
8	7	-5554.38	-5532.67	0.11	-5554.41	-5532.51	-0.02
	8		-5532.61	0.17		-5532.39	0.11
	12		-5533.20	-0.41		-5532.61	-0.12
	13		-5532.98	-0.19		-5532.26	0.24
9	8	-5554.21	-5532.44	0.17	-5554.24	-5532.31	0.01
	9		-5532.65	-0.03		-5532.50	-0.18
	18		-5532.42	0.19		-5532.33	-0.01
	25		-5532.42	0.20		-5532.31	0.01
10	9	-5554.37	-5533.09	-0.30	-5554.41	-5532.60	-0.11
	10		-5532.96	-0.17		-5532.42	0.07
	15		-5532.52	0.27		-5532.36	0.13
	26		-5532.55	0.24		-5532.42	0.07
11	10	-5554.21	-5532.86	-0.24	-5554.25	-5532.29	0.04
	11		-5532.55	0.08		-5532.32	0.00
	14		-5532.74	-0.11		-5532.25	0.08
	22		-5532.56	0.06		-5532.37	-0.04
12	11	-5554.25	-5532.71	-0.04	-5554.28	-5532.38	-0.01
	12		-5533.16	-0.50		-5532.52	-0.15
	20		-5532.48	0.19		-5532.38	-0.01
	24		-5532.36	0.31		-5532.24	0.13

[a] Both absolute and relative values are given in eV. Al, Al-O_H, and proton energies (-PA) are given in eV for formal charge *differences* (see Table III) with respectively full-range O_H potentials and truncated ones.

Table IX[a]

substitution site		force field (dQ = 0.5)					
		full range			truncated		
Al	O_H	E(Al)	E(Al-O_H)	-PA	E(Al)	E(Al-O_H)	-PA
1	1	-5553.37	-5541.21	-0.17	-5553.63	-5540.92	0.16
	15		-5540.67	0.37		-5540.89	0.19
	16		-5541.67	-0.64		-5541.54	-0.46
	21		-5540.56	0.47		-5540.84	0.23
2	1	-5553.36	-5541.26	-0.24	-5553.63	-5540.94	0.14
	2		-5540.37	0.66		-5540.67	0.40
	6		-5541.16	-0.13		-5541.35	-0.27
	13		-5541.79	-0.76		-5541.22	-0.14
3	2	-5553.38	-5540.36	0.68	-5553.65	-5540.67	0.42
	3		-5541.55	-0.50		-5541.17	-0.08
	19		-5541.30	-0.26		-5541.30	-0.21
	20		-5540.66	0.39		-5540.96	0.13
4	3	-5553.43	-5541.78	-0.69	-5553.74	-5541.20	-0.02
	4		-5540.98	0.12		-5540.89	0.29
	16		-5541.72	-0.63		-5541.57	-0.39
	17		-5541.20	-0.11		-5541.28	-0.10
5	4	-5553.32	-5540.87	0.12	-5553.57	-5540.92	0.10
	5		-5540.45	0.54		-5540.74	0.27
	14		-5541.16	-0.17		-5541.25	-0.23
	21		-5540.47	0.52		-5540.76	0.25
6	5	-5553.33	-5540.43	0.56	-5553.58	-5540.74	0.29
	6		-5541.44	-0.45		-5541.31	-0.29
	18		-5540.44	0.55		-5540.75	0.28
	19		-5541.33	-0.34		-5541.26	-0.24
7	7	-5553.40	-5540.89	0.17	-5553.67	-5541.14	-0.03
	17		-5541.29	-0.23		-5541.24	-0.13
	22		-5540.87	0.20		-5541.10	0.01
	23		-5540.54	0.52		-5540.82	0.29
8	7	-5553.38	-5540.88	0.17	-5553.68	-5541.15	-0.03
	8		-5540.81	0.23		-5540.97	0.15
	12		-5541.66	-0.61		-5541.57	-0.45
	13		-5541.62	-0.58		-5541.23	-0.11
9	8	-5553.38	-5540.92	0.12	-5553.63	-5541.03	0.05
	9		-5541.67	-0.63		-5541.60	-0.52
	18		-5540.48	0.56		-5540.79	0.28
	25		-5540.94	0.10		-5540.88	0.20
10	9	-5553.40	-5541.58	-0.51	-5553.68	-5541.61	-0.48
	10		-5541.43	-0.36		-5541.35	-0.23
	15		-5540.66	0.41		-5540.91	0.22
	26		-5540.72	0.35		-5541.02	0.11
11	10	-5553.34	-5541.37	-0.36	-5553.62	-5541.28	-0.21
	11		-5540.82	0.19		-5540.96	0.11
	14		-5541.25	-0.24		-5541.07	0.00
	22		-5540.81	0.20		-5541.03	0.04
12	11	-5553.39	-5540.97	0.09	-5553.66	-5541.04	0.06
	12		-5541.72	-0.66		-5541.58	-0.48
	20		-5540.66	0.40		-5540.94	0.16
	24		-5540.49	0.57		-5540.78	0.32

[a] As Table VIII, but for half formal charge *differences*.

proton energy predictions and the width of the PA distribution. Once these have been established, it is worthwhile to search a relation between PA and the crystal structure. It appeared that proton affinity of an AlO_H substituent is correlated with the interatomic distances (TO and OO) of the all-silica lattice. This interdependence is the same for FAU and MFI. In this section we will focus on MFI, since for this zeolite the large number of crystallographically different substitution sites makes a statistical treatment of data meaningful.

Figure 9 shows the interdependence between proton energies of the various oxygen sites in MFI and the average Si–O and O–O distances. The proton is best accommodated (i.e., the energy is lowest and the PA highest) at those oxygen sites which have relatively large Si–O distances and relatively short O–O distances.

This relation between structure and proton affinity is in line with physical intuition: since the TO_H bonds are substantially longer than the TO bonds, long TO bonds provide a favorable starting point. Additionally, it was found that sites with large TO distances have relatively small OO distances. This implies that the OTO angles at oxygen sites that bind the protons best are small, which again favors proton attachment, since, upon protonation, the optimum O_HTO angle is 90–100°, rather than the normal tetrahedral angle of 109.47°.

One also observes (Figure 9) that the correlation between PA and the Si–O–Si angle is much weaker than the correlation with the distances. This is rationalized by the fact that the unprotonated TOT angle is very flexible and hence its variation does not influence the energy very much. We note in passing that these observations are inconsistent with the hypothesis of Dwyer et al.,[4,5] who claim—on the basis of cluster calculations—that the TOT angle is an important factor in determining the acidity of sites.

A correlation between PA, which is a property of the *substituted* lattice, and the structure of the *unsubstituted* lattice implies the

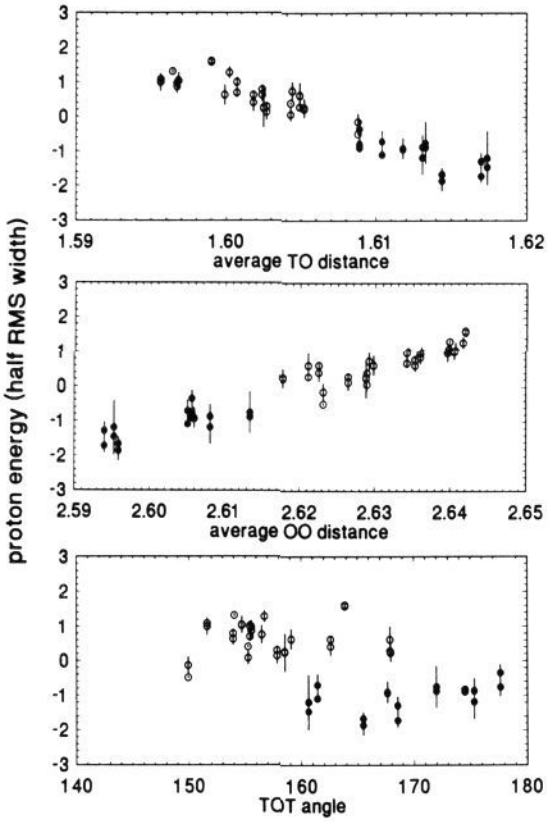

Figure 9. Relation between average T–O distance, O–O distance, and T–O–T angle in the relaxed all-silica structure of MFI, and the (averaged) proton energy of corresponding oxygen site. A distinction is made between oxygen atoms that are part of one of the 10-rings spanning the MFI channels (○) and atoms that are not in those rings (●).

effect of lattice relaxation (in particular the relaxation energy) is more or less the same for all oxygen sites, as is indeed observed. This is shown in Figure 10, where the relative energies of substitution at various sites before and after relaxation are compared. The straight line with unit slope implies site-independent relaxation energy. The constancy of the relaxation energy would imply that the distortion of the lattice extends over a sphere of such dimensions and that local geometrical, lattice-topological differences and anisotropies are washed away.

A numerical argument in favor of this hypothesis comes from *the decay of the lattice distortion around an AlO_H substitution.* Figure 11 shows the scatter diagram of the change in TO bond lengths in MFI (δ_{TO}) upon the introduction of an AlO_H substitution in an all-silica lattice versus the distance from the substitution (taken as the O_H site). One observes an approximately exponential decay of δ_{TO} with distance

$$\delta_{TO}(r) = \delta_0 \exp(-r/\lambda) \qquad (5)$$

with $\lambda \approx 3.3$ Å. Assuming that the distortion energy is proportional to the square of the displacement and taking the continuum limit, we can calculate the total lattice distortion energy $E_d(R)$ within a sphere of radius R from the substitution:

$$E_d(R) = \int_0^R \delta_{TO}(r) \qquad (6)$$

The latter function is plotted as an insert in Figure 11, from which one sees that the distortion energy is spread out over a large sphere with a 5–10 Å radius, which is quite large in comparison with the unit cell dimensions.

For MFI, besides a correlation between PA and interatomic distances, it was found that there is a correlation between PA (and the interatomic distances) and the location of oxygen atoms

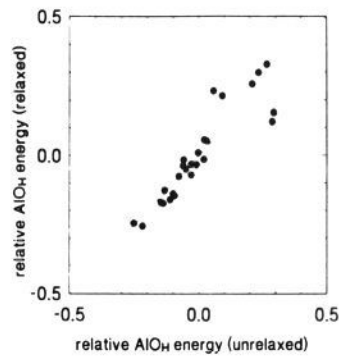

Figure 10. Correspondence between AlO_H substitution energies in the all-silica structure and the energy of the relaxed structure. The high degree of correlation indicates a constant relaxation energy. Results were obtained with the $\delta Q = 1$, full-range force field.

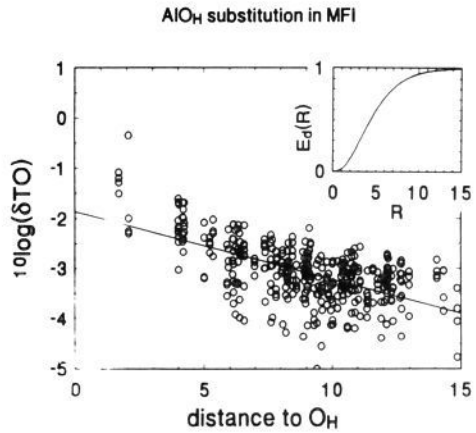

Figure 11. Change in the TO interatomic distances upon AlO_H substitution in the all-silica MFI framework, plotted versus the distance from the O_H substituent. The insert shows the integrated distortion energy (according to eq 6) of the substituent versus the radius of the integration sphere.

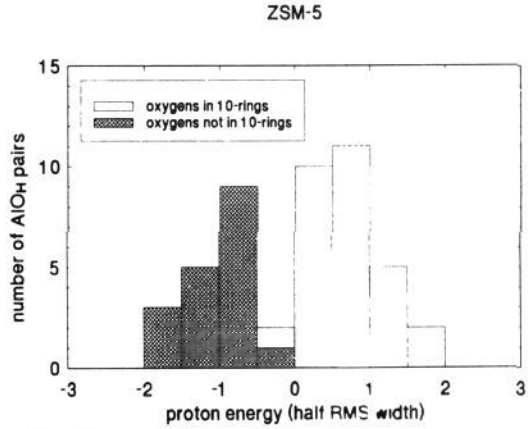

Figure 12. A histogram of the averaged and scaled proton energies for MFI. A distinction is made as to whether or not protons are on oxygens that are part of one of the 10-membered rings that form the channels. See also Table X.

on one of the 10-membered rings that surround the MFI channels. Oxygen sites that occupy positions in these rings are unfavorable for proton attachment in comparison to sites that do not participate in one on the 10-rings. This effect is shown in Figure 12 as two distribution functions. In fact the effect is so strong that the distribution of PA is bimodal, consisting of two distributions that hardly overlap.

The relation that we have established between PA and the structure of the unsubstituted lattice, in combination with the fact that the results for PA differences are retained, even if the

Table X. Structural Analysis of ZSM-5[a]

	proton position				
	S-channel		Z-channel		
O-site	ring	conn	ring	conn	interior
1	x			x	
2	x		x		
3				x	
4			x		
5	x		x		
6				x	
7	x				
8	x				
9				x	
10				x	
11	x				
12					x
13		x			
14		x			
15			x		
16					x
17			x		
18	x		x		
19		x			
20	x		x		
21	x			x	
22	x				
23		x	x		
24		x	x		
25		x	x		
26			x		

[a] O-sites are numbered after Olson et al.[26] For each O-site, we have indicated whether or not it is on the inner surface of one of the channels. For O-sites on the inner surface of one of the channels it is indicated whether it is part of one of the 10-rings that surround the channels (*ring*), or whether it forms the connection between two of those rings (*conn*). *S-channel* is the straight channel along the *b*-axis; *Z-channel* denotes the zigzag channel along the *a*-axis and *interior* indicates that the oxygen site is not on the surface of either of the main channels.

short-range force field is truncated and if charge differences are halved, implies that the reliability of PA predictions is for a large part determined by the reliability of the all-silica force field. In previous work,[20] we have shown that our force field does provide a reliable description of the all-silica lattice. Even so, we cannot be absolutely confident that the small differences in TO and OO distances and OTO angles, which appear to determine the proton affinity of different crystallographic sites, are predicted with a sufficient degree of accuracy. The correspondence between theory and experiment for FAU is hopeful, but experimental confirmation for another framework would be very helpful at this point.

The structure–acidity relationship provides—a posteriori—a rationale for the averaging of data of different sets of force fields. Since the larger part of the PA variation has—for all force fields—its origin in the variation of distances and angles of the all-silica lattice, the relative differences are identically predicted, and only the width of the PA distribution is force field dependent.

In conclusion, the relationship between PA and structure found here is a valuable tool and should be studied in more detail in order to further establish its validity. If validated, it provides us with a useful and simple tool to assess the acidity of zeolites. In that case it should be possible to predict the acidity of specific sites from accurate (!) crystal structure data.

3.4. Summary of Results. We have obtained a method for predicting the spectrum of PA differences in zeolites due to structural differences. The width of this distribution of proton affinities is the same for FAU and MFI. Our best estimate for this width is 0.8 eV. This value is close to estimates found in the literature as can be seen from the summarizing Table XI.

The magnitude of PA differences in this paper is influenced by the radius of the sphere around the AlO_H substitution that is allowed to relax. The larger this radius, the larger the differences. In spite of the variation of these estimates, it is obvious that these

Table XI

	range of PA difference (eV)	
ref	FAU	MFI
this work	0.8	0.8
Schröder[13,14]	0.25	0.35–0.50[a]
Dubský[15]	0.6	

[a] The magnitude of PA differences in this paper is influenced by the radius of the sphere around the AlO_H substitution that is allowed to relax. The larger this radius, the larger the differences.

0.5–1 eV differences are of the same order of magnitude as the PA differences induced by chemical differences in the zeolite (low-Al versus high-Al), which run up to 1 eV, making both factors competitive, and rationalizing the large variation in catalytic activity found for different zeolitic frameworks of equal chemical composition.

The detailed prediction of high- and low-acid sites proved possible for zeolite FAU, for which all force field predictions of all authors coincide. Additionally there is experimental evidence to justify the outcome of these calculations: sites that are predicted to be energetically favorable are found to be occupied in neutron diffraction experiments. For MFI the results are more sensitive to changes in the force field.

In all data there appears to be a correlation between acidity and structure, viz., the TO and OO distances of the all-silica lattice. Therefore, the reliability of acidity predictions is primarily determined by the reliability of the force field that describes the all-silica lattice, and further work in this area should therefore be concentrated on the assessment (and if necessary, improvement) of the reliability of the prediction of interatomic distances in SiO_2 lattices.

4. Summary

In this paper we have studied the "intrinsic acidity" of zeolites through quantum-chemical and force field type techniques. We have established the acidity differences in terms of energy differences for proton abstraction.

The work presented in section 2 is based upon earlier work[11] where it was shown that geometry-optimized zeolitic clusters are good model systems for the extended zeolite. Therefore geometry-optimized clusters can be used to assess the influence of chemical composition on zeolite acidity. A systematic study of all possible $(Si,Al)O_2$ 4-ring conformations showed that protons are invariably bound to oxygen atoms of the Al–O–Si type. Violation thereof requires over 2 eV, or 190 kJ/mol. This implies that acidity differences are determined by differences in the chemical or structural embedding of this unit. Chemical differences in the second coordination sphere of T-atoms surrounding the acid OH group induce differences of approximately 0.5 eV in 4-rings, but this effect might be amplified to 1 eV in a real zeolite, because of the larger T-atom coordination number.

Structural differences were studied with force field methods, using a force field derived in a previous study.[11] It was found that for low-aluminum zeolites structural differences induce a variation in the proton affinities between the four inequivalent oxygen sites that surround an aluminum substitution, which may be as large as 0.8 eV. For zeolite Faujasite, the outcome was in agreement with an experimental determination of preferred proton siting. The wealth of theoretical data obtained for ZSM-5 allowed us to establish a relationship between PA and the SiO and OO interatomic distances of the all-silica lattice.

Both chemically and structurally induced proton affinity differences are mainly due to differences in the covalent bonding strengths between the acid group and neighboring T-atoms, which may vary either as a result of chemical substitution or through the stretching or compression of bonds due to embedding.

Appendix I: Truncation of the Al–O_H Force Field

A systematic error in the force field predictions for substitution energies occurs as a consequence of its functional form, which specifies interactions primarily in terms of nonbonded interactions (eq 2). In a previous paper[11] we have shown that the force field predictions for the lattice energy of SiO_2 polymorphs depends on the density of the polymorphs. It was shown that this is a spurious consequence of the functional form of the force field.

Force-field parameters have been determined in such a way that they yield a proper description of the equilibrium *forces* between atoms, thus ensuring the optimal prediction of structural and elastic properties of SiO_2 polymorphs.[20] In practice this means that a single short-range term describes both the covalent and the nonbonded interactions between atoms. As a result, the c-values used in the force field have numerical values that are higher than appropriate to describe the van der Waals interaction. Since the r^{-6} terms are all additive, their total contribution is dependent on the framework density. Once the origin of the suprious density dependence was clarified, a scheme was set up to correct for it. We will now analyze the situation with respect to substitution energies.

The r^{-6}-term also causes a spurious density dependence of the substitution energy differences between different O-sites in a zeolite, because the *local density* varies between O-sites. By local density we mean the number of T-atoms in the vicinity of an O-atom or O_H-group. To quantify this statement, it is useful to consider the quantity ($\tilde{n}_i(R)$), defined as

$$\tilde{n}_i(R) = \sum_{j:r_{ij}>R} \frac{1}{r_{ij}^6} \tag{7}$$

where i is an O-site and j are T-sites. Clearly $\tilde{n}_i(R)$ is different for all O-sites. In particular it depends on the local topology of 4-, 5-, and 6-rings. Upon replacement of O by O_H we have a contribution to the substitution energy that is proportional to

$$(c_{SiO_H} - c_{SiO})\tilde{n}_i(R) \tag{8}$$

As the c-values are calibrated for clusters only, the contributions from terms in eq 7 with $r_{ij} \geq 3.5$ Å are spurious and the resulting systematic error is approximately

$$(c_{SiO_H} - c_{SiO})\tilde{n}_i(3.5) \tag{9}$$

a quantity that may exceed 0.1 eV. As this is of the same order of magnitude as the energy differences that we are interested in, we should make a correction for it.

This can be done by changing the range of the force field parameters. A sensible choice is to describe an O_H substituent by O_H parameters for the interactions with neighboring Si and O atoms only ($r_{ij} < 3.5$ Å), and by regular O parameters for atom pairs with $r_{ij} \geq 3.5$ Å. This implies that beyond the nearest neighbor distance, the O_H substituent behaves as an O-atom except for its charge. In doing so, one eliminates the spurious density dependence of the force field results.